Deflection Behaviors of Polymer Mortar Sandwich Panels Reinforced with GFRP

Kyu-Seok Yeon, Jaichul Yi, Hyun-Jong Lee

Regional Infrastructure Engineering Program, Kangwon National University, Chuncheon 200-701, Korea

Received 31 January 2007; accepted 29 November 2007
DOI 10.1002/app.27799
Published online 23 January 2008 in Wiley InterScience (www.interscience.wiley.com).

ABSTRACT: This study prepared sandwich panel specimens composed of methyl methacrylate (MMA)-modified polymer mortar at the core and reinforced with high-tensile GFRP on both faces to propose a method to predict the deflection of polymer mortar sandwich panels under flexural load. Nine experimental specimens of different thickness at the core and face were prepared for the flexural load test to determine the moment-deflection relationship, and the experimental results were compared with existing theoretical models. The comparison study revealed that the deflection behavior of the specimens in response to the variation in the thickness of the specimens at the core and face could be well predicted. Additionally, an analytical model, which revised a bilinear method, to explain the tension stiffening effect of the prepared sandwich panel specimens under the influence of flexural load is proposed. © 2008 Wiley Periodicals, Inc. J Appl Polym Sci 108: 1336–1347, 2008

Key words: composites; mechanical properties; reinforcement; fiber

INTRODUCTION

The structural built-up of polymer mortar sandwich panels reinforced with glass fiber-reinforced polymer (GFRP) developed in this study is basically the same as the structure of existing sandwich panels, but its material composition is different. Because the existing sandwich panels use a weaker and sparse core, the flexural rigidity of the core is overlooked.[1] Moreover, the moment of inertia increases to result in greater stiffness of the structure as the face is distanced from the neutral axis. Nevertheless, since the polymer mortar used as the core of this study has excellent strength, it can contribute to the moment of inertia as well as to strength. Thus, the flexural rigidity of polymer mortar at the core must be carefully accounted for in the design and analysis of the polymer mortar sandwich panels.

The field application of polymer mortar sandwich panels reinforced with GFRP with these properties must be examined in terms of material and structural characteristics.[2] The material aspect of the polymer mortar must determine the influence of the compositional element on the strength manifestation and the mechanical properties of compressive strength, tensile strength, and the modulus of elasticity, as well as creep and dry shrinkage properties. In addition, the structural aspect must examine the change in moment-deflection relationship, resistance moment, and flexural rigidity in response to the thickness of the polymer mortar at the core and the thickness of the reinforcing GFRP.

Reinforced members subjected to bending are characterized, when the flexural moment is greater than the first cracking moment, by the crack deformation. The cracking leads to transferring of the tensile load to the reinforcing parts while the reinforced member between two consecutive cracks is still reacting. This effect is usually referred to tension stiffening.[3]

Several theoretical models have been used to take account of the tension stiffening and to predict the moment-deflection behaviors after the first crack. ACI Building Code[4] and the Canadian Building Code[5] proposed methods to estimate the immediate deflection using a constant effective moment of inertia. For most of the concrete members reinforced with FRP bars, the deflection is currently predicted by the model proposed by ACI Committee 440.[6] This committee modified the gross effective moment of inertia of the cross section as described in the ACI Building Code by taking account the modulus of elasticity of the FRP material, the modulus of elasticity of the reinforcing steel, and the bonding condition. The model was successfully applied to various types of FRP bars.[7,8] The code suggests a member-dependent modification constant[6] to estimate long-term deflection of Aramid fiber-reinforced polymer bars, glass-fiber reinforced polymer bars, and carbon-fiber reinforced polymer bars. Hall and Ghali[9] introduced the mean moment of inertia by which

Correspondence to: J. Yi. (jyi@kangwon.ac.kr).
Contract grant sponsor: Ministry of Construction and Transportation.

Journal of Applied Polymer Science, Vol. 108, 1336–1347 (2008)

the mean curvature of the beams reinforced with GFRP bars rather than the effective moment of a flexural member was calculated. The mid-span deflection was computed by integrating the mean curvature at a number of sections along the member. Similar integration method was also suggested by Razaqpur[10] and Razaqpur et al.[11] Following CEB-FIP Model Code 1990,[12] Favre and Charif[13] proposed an instantaneous deflection equation named the bilinear model to compute the deflection of ordinary reinforced concrete. The model assumes the following: the tension stiffening effect of concrete on curvature of any section of a flexural member decrease with the actions increasing beyond the reduced cracking moment.[12] It will be interesting subject that if the moment-deflection behaviors of the sandwich panels produced in this study agree with the predictions of aforementioned theoretical models. The authors believe that it will be an interesting research topic itself to investigate whether the flexural behavior of the sandwich panel developed in this study agrees with the moment-deflection as predicted by the aforementioned theoretical models.

Specimen of methyl methacrylate (MMA)-modified polymer mortar at the core and reinforced with high-tensile GFRP at both faces were prepared for this study. This polymer mortar sandwich panels reinforced with GFRP were then subjected to flexural tests. Additionally, the experimental results of the change in moment-deflection relationship and flexural rigidity in response to the various thickness of the polymer mortar at the core and the various thickness of the reinforcing GFRP at the face were analyzed and compared with the values computed from existing prediction models.

RESEARCH SIGNIFICANCE

The experimental results pointed at the tension stiffening effect as evidenced by the deflection behavior of the sandwich panel, of which the modulus of elasticity at the core was greater than that at the face. The existing model was revised to propose a new model to compute the deflection of the sandwich panels under short-term static load. This proposed model was compared against other models in terms of the computational predictability based on the experimental data. This research finding is believed to be very useful as guideline for the design of polymer mortar sandwich panel structures reinforced with GFRP.

EXPERIMENTAL

Materials

The binder is composed of a mix of UP resin and MMA at the weight ratio of 7 : 3. A dimethyl phthalate (DMP) solution of 55% methyl-ethyl-ketone peroxide (MEKPO) and *N*,*N*-dimethylaniline (DMA) were used as initiator and promoter for MMA and UP resin, respectively.

UP resin markedly shrinks by 7–10% during hardening. This shrinkage varies with the content of styrene monomer in the resin regardless of the hardening time. Thus, this study used a shrinkage-reducing agent (SRA) made by dissolving thermoplastic polystyrene into styrene monomer to reduce the shrinkage.

The major objective of using fine-grained filler in the polymer concrete mix is to decrease the amount of resin per unit volume and to improve the viscosity. Although round grains are better in increasing the weight, the granules with irregular shape are more advantageous in improving the viscosity because of this greater specific surface area.

There are many kinds of fillers, but this study opted for calcium carbonate. Calcium carbonate is obtained from crushing limestone and is inexpensive and easily available. Moreover, its absorptivity of polymer resin is relatively small, which is advantageous for the mix. There are heavy and light kinds of calcium carbonate. Considering the workability of polymer concrete, heavy calcium carbonate is appropriate, and thus calcium carbonate of 1- to 30-μm particle size, 2.5–3.0 m^2/kg in fineness, and water content of below 0.1% was chosen for the study.

Generally, when an aggregate with hydrophilic property in polymer concrete starts absorbing water, a water membrane is formed between the surface of the aggregate and the binder around the aggregate in the polymer concrete. This makes the bonding between the binder and the aggregate weaker and lowers the strength of the concrete. Thus, the polymer concrete aggregates need to be dried so that the water content of calcium carbonate should be below 0.1% by weight. This study used dried silica sand (No. 6 and Special No. 1) to make its water content below 0.1% before using it as the fine aggregate.

Relatively thick E-glass textile fabric was used as the reinforcing glass, and a roving cloth rather than a mat was used so that it can make the thickness of the FRP-reinforced concrete more uniform.

The physical and chemical properties of the materials used in this study are shown in Table I.

Specimens

Polymer mortar for core

Because the mix for polymer mortar varies according to the purpose of the use, the resin type, aggregate form and density, working conditions, etc., the optimum mix proportion is determined by maximizing the content of the aggregate and filler, and by mini-

TABLE I
Properties of Used Materials

UP resin			
Density (25°C)	Viscosity (25°C, mPa s)	Acid number	Styrene content (%)
1.13	300	20.0	40

MMA			
Density (20°C)	Viscosity (20°C, mPa s)	Molecular weight (g/mol)	Appearance
0.9420	0.56	100	Transparent

Initiator		
Component	Density (25°C)	Active oxygen
MEKPO 55%, DMP 45%	1.12	10.0

Promoter				
Density (20°C)	Boiling point (°C)	Melting point (°C)	Molecular weight (g/mol)	Appearance
0.956	193–194	1.5–2.5	121.18	Oily liquid

Shrinkage reducing agent		
Density (25°C)	Nonvolatile matter (%)	Appearance
31–41	34–38	Transparent

Ground calcium carbonate					
Density (g/cc)	Absorption (cc/g)	Water content (%)	pH	Mean grain size (μm)	Retained percentage of 325 meshsieve
0.75	0.20	0.3	8.8	13	0.03

Ground calcium carbonate (chemical component)					
CaO	Al_2O_3	Fe_2O_3	SiO_2	MgO	Ignition loss
53.7	0.25	0.09	2.23	0.66	42.4

Fine aggregate					
Size (mm)	Apparent density	Bulk density	Unit weight (kg/m^3)	Fineness modulus	Absorption (wt %)
5	2.62	2.6	1,645	2.48	0.44

Roving cloth				
Count (yarns/inches)		Weave	Weight (kg/m^2)	Width (mm)	Thickness (mm)
Warp	Fill				
6.3	6.3	Plain	0.58	1000	0.6

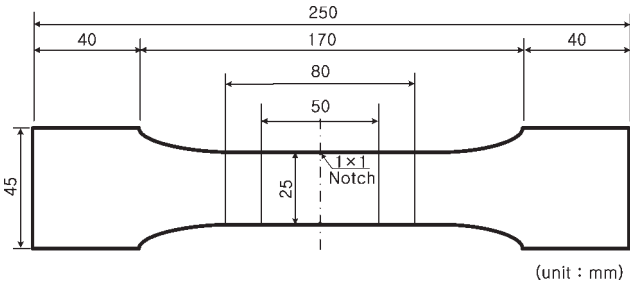

Figure 1 Details of GFRP tensile specimen.

mizing the content of polymer binder within the experimental boundary of workability and strength.

Unsaturated polyester resin is the most widely used binder for polymer concrete (mortar) for its excellent performance to the cost ratio. However, decrease of workability is often happening due to the high viscosity of unsaturated polyester resin. A relatively large amount of binder is then required to attain good workability.

This study used a MMA-modified polymer mortar, which is obtained by adding MMA to unsaturated polyester resin, to reduce the amount of binder, and to improve workability. The viscosity of UP resin and MMA used as binder is 300–400 mPa s and 0.56 mPa s, respectively, indicating that the viscosity of MMA is much lower than that of unsaturated polyester resin. Thus, the viscosity of binder obtained by adding MMA to unsaturated polyester resin is lowered by the amount of added MMA, and improvement in workability and reduction in the amount of the binder can be achieved through the addition of MMA. However, there will be problems of material separation and bonding reduction if MMA is added more than the optimum amount. Thus, the optimum mix proportion for the binder is determined by several trial-and-error runs.

The specimen for strength tests were prepared in accordance with the specification of BS 6319-1 : 1983.[14] A mold of Φ75 mm × 150 mm was used as specimen for the compressive and wedge splitting tensile strength test, and a mold of 60 mm × 60 mm × 240 mm was used as specimen for the flexural strength test. The specimens were prepared and stored at 20°C ± 2°C. The specimens were compacted in three layers. Each layer was compacted with 25 hits with a rod of 12 mm diameter and 300 mm length, and the outside of the specimen was compacted with a vibrator of 3000 rpm for about 2 min after the inside compaction. The prepared specimens were cured for 7 days in a curing room kept at the temperature of 20°C ± 2°C and relative humidity of 60%.

GFRP for facings

This study employed a hand lay-up method, because it makes the specimen preparation easier and cheaper regardless of the specimen size. The GFRP is formed by cutting the roving cloth appropriate for the mold size. Then, it is placed in the mold, and the binder prepared by mixing MMA to unsaturated polyester resin is added by each layer until it reaches the desired thickness. The binder used at this time is the same binder as the MMA-modified polyester mortar, and the weight ratio of the glass fiber to the binder was set to 1 : 0.92.

The thickness of the test specimen was varied to five kinds (0.5, 1.5, 2.0, 2.5, 3.35 mm) in the shape of a panel initially, and then they were processed precisely to satisfy the shape of specimen as specified by BS 2782-9[15] with a milling cutter. Figure 1 shows the details of the facial GFRP specimen with its shape and size.

Polymer mortar sandwich panel reinforced with GFRP

The thickness of the GFRP reinforcement at the face was varied by 1.5, 2.0, and 2.5 mm in the preparation of the MMA-modified polymer mortar sandwich panel reinforced with GFRP. The MMA-modified polymer mortar at the core was prepared and placed in accordance with the previously determined polymer mortar mix proportion pursuant to the specification of BS 6319-1.[16] The size specification for the sandwich panel specimen prepared in this study is shown in Table II. Because previous sandwich panels used core of weak strength and sparse density, it ignored the flexural strength at the core and only enhanced the strength by increasing the second moment of inertia of the cross section owing to the face distanced from the neutral axis. Nonetheless, the polymer mortar used as the core in this study has excellent strength itself and exerts positive influence on the attainment of moment of inertia and the strength manifestation. Because the compressive strength of FRP is much weaker than the tensile strength in general, the reinforcement at the compressive side does not greatly affect the flexural strength. Thus, this study opted to use the reinforcement of the same thickness for the compressive side and the tensile side for esthetic consideration and to prevent brittle failure at cracking.

Test methods

Polymer mortar for core

The compressive (flexural) strength test followed the method specified by BS 6319-2[17] (BS 6319-3[18]) and used the cylindrical (square prismatic) specimen of Φ75 mm × 150 mm (60 mm × 60 mm × 240 mm). A cylindrical specimen was used for the tensile strength test pursuant to BS 6319-7.[19] The modulus of elasticity

TABLE II
Details of GFRP-Reinforced Polymer Mortar Sandwich Panels

Specimens	Length (mm)	Width (mm)	Core thickness (mm)	Facing thickness	
				Tensile side (mm)	Comp. side (mm)
T3-1.5	1,200	300	30	1.5	1.5
T3-2.0				2.0	2.0
T3-2.5				2.5	2.5
T4-1.5	1,200	300	40	1.5	1.5
T4-2.0				2.0	2.0
T4-2.5				2.5	2.5
T5-1.5	1,200	300	50	1.5	1.5
T5-2.0				2.0	2.0
T5-2.5				2.5	2.5

was measured in accordance with BS 6319-6,[20] and the size of the specimen was Φ75 mm × 150 mm.

GFRP for facings

The tensile strength test for GFRP reinforcement at the face of the specimen was carried out after making a GFRP panel with five layers of roving cloth laid up layer by layer. Then, the test specimen was prepared and the tensile modulus of elasticity was measured in accordance with BS 2782-9.[21]

GFRP-reinforced polymer mortar sandwich panel

The flexural strength test for polymer mortar sandwich panel reinforced with GFRP was carried out in accordance with three-point loading method as specified by JIS A1414.[22] Figure 2 illustrates the loading test for the sandwich panel. Loading was applied until the specimen was fractured while rigid rubber packing was inserted between the loading plate and the specimen to alleviate the local contact stresses. Additionally, two strain gauges were installed at the center of the composite panel on the tensile side and compressive side to measure the strain on the panel due to the loading. Moreover, a linear variable displacement transducer (LVDT) with 0.05-mm precision at the direction of the loading was installed to measure the deflection. Figure 3 depicts the location of the strain gauges installed to measure the strain on the sandwich panel during flexural test.

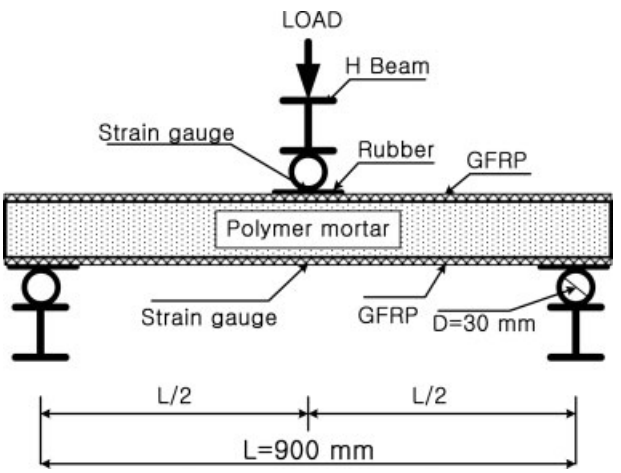

Figure 2 Schematic sketch of three-point flexural test.

RESULTS AND DISCUSSION

Physical and dynamic properties of composite materials

Polymer mortar for core

The average compressive strength was 100.0 MPa based on the compressive tests on 15 cylindrical specimens of Φ75 mm × 150 mm. This is in the same order of magnitude as the existing polymer mortar with unsaturated polyester resin binder. The average flexural strength was 23.5 MPa based on the flexural strength tests on 15-square prismatic specimens of 60 mm × 60 mm × 240 mm. Considering that the flexural strength of ultra-high strength cement concrete with compressive strength of about 118 MPa is between 9.2 and 11.5 MPa, this value indicates that the flexural strength of MMA-modified polyester polymer mortar is very high. The average tensile strength was found to be 13.5 MPa based on

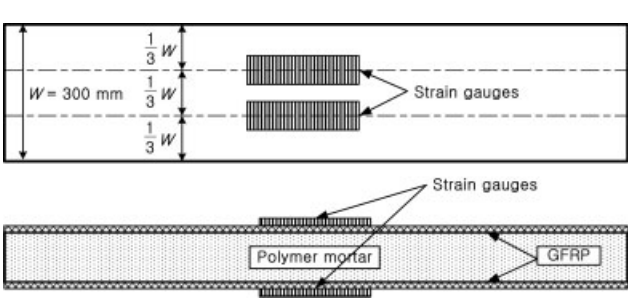

Figure 3 Instrumentation of strain gauge for flexural test.

TABLE III
Measured Physical Properties of Polymer Mortar and GFRP

Polymer mortar					
Compressive strength (MPa)	Flexural strength (MPa)	Tensile strength (MPa)	Elastic modulus (MPa)	Ultimate stress (MPa)	Ultimate strain (%)
100.0	23.5	13.5	2.2×10^4	100.0	0.8

GFRP		
Tensile strength (MPa)	Elastic modulus (MPa)	Tensile elongation at break point (%)
302.8	1.0×10^4	3 ± 0.05

the tensile strength tests on 15 cylindrical specimens of Φ75 mm × 150 mm.

The modulus of elasticity was obtained from the secant modulus of elasticity based on the stress–strain curve at the loading up to 40% of the fracture load. The average ultimate stress was 100.0 MPa as computed from compressive stress–strain curve, and the ultimate strain was about 0.008, which is about 2.7 times the ultimate strain of ordinary cement concrete, 0.003. Additionally, the modulus of elasticity at the stress 40% of the ultimate stress was 2.2×10^4 MPa. This is a very low value as compared with 4.0–4.4×10^4 MPa, which is the typical modulus of elasticity for high-strength cement concrete with compressive strength of 100–127 MPa. The top of Table III summarizes the physical properties of polymer mortar at the core as measured in this experiment. Figure 4(a) shows typical stress–strain curves for the polymer mortar core.

GFRP for facings

The average tensile strength of GFRP for the facings of the polymer mortar sandwich panel specimen was 302.8 MPa. The average tensile modulus of elasticity was 1.0×10^4 MPa for the reinforcing GFRP based on the experimental results. This is about half of the modulus of elasticity for MMA-modified polyester polymer mortar (2.2×10^4 MPa). Generally speaking, concrete exhibits almost linear and elastic stress–strain relationship only during the early loading stage and curvilinear stress–strain relationship beyond the loading greater than 40–50% of the ultimate load. Nonetheless, GFRP manifested almost linear stress–strain relationship even beyond the loading greater than 40–50% of the ultimate load, and this behavior continued until the specimen was fractured. In addition, the tensile elongation at break point of the specimens was almost the same at 3% ± 0.05% regardless of the thickness of GFRP. The bottom of Table III summarizes the physical properties of GFRP as measured in this experiment. Figure 4(b) is the stress–strain curve for the GFRP facings.

Deflection behavior of polymer mortar sandwich panel

Ever since steel reinforced concrete has been used as a structural material, design theories and methods

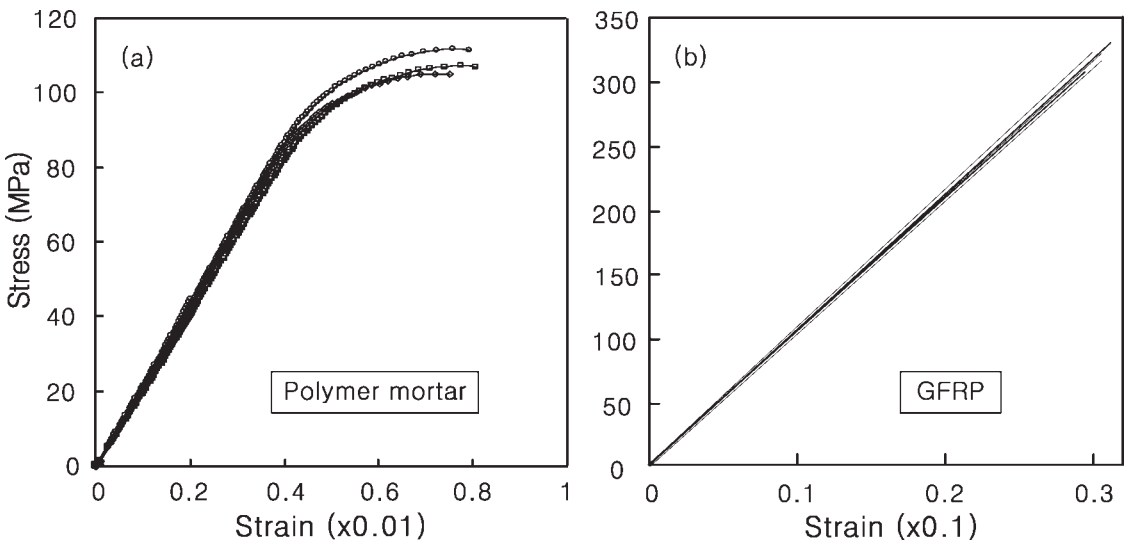

Figure 4 Stress–strain curves (a) for polymer mortar core and (b) for GFRP facings.

have been developed continuously. Once these theories and methods were limited to elastic property, but now they have been expanded to cover inelastic behavior. Design theories for flexural members such as reinforced concrete beam and slab are based on the following basic assumptions. First, the strain on the steel inside the concrete is the same as the strain on the concrete surrounding the steel. Second, the cross section plane prior to loading maintains the plane shape even after loading. Third, because the tensile strength of concrete is very low and the tensile elongation of concrete is very small compared with steel, cracking takes place at the tensile side of concrete in general. Fourth, the recent theory on steel concrete is based on the stress–strain relation and the strength property of the two composing materials or rational simplification of such relationship and property.

Based on these basic assumptions, the stress on such flexural members as beam and slab are borne by concrete at the compressive side of the neutral axis and reinforcing steel at the tensile side of the neutral axis. In addition, as the load increases, the following series of yield behavior is accompanied by each stage. Cracks take place at the concrete on the tensile side, the neutral axis moves, the stress inside the structure is redistributed, the steel yields, and the structure reaches the final failure. In addition, the ductility index as computed from the load-deflection curve or moment-curvature curve of the flexural tests for reinforced concrete beam and slab as well as the equivalent stress block model for concrete as obtained through the eccentric compressive tests for C-type beam can explain the behavior of the flexural members and the characteristics of the stress distribution by numerical analysis methods. These approaches are all appropriate for the design and analysis of flexural members.

On the other hand, the thin panel members are subject to bending, and the formation and movement of the neutral axis in response to the load increase and redistribution of the stress inside these members are hard to determine by experiment. Additionally, as it is mentioned earlier, the core material of the specimen used in this study is of polymer mortar with lower elastic modulus compared with its compressive and flexural strength, and the facings of the specimen are reinforced by GFRP with high-tensile property (16–30 times that of polymer mortar) and high-tensile elongation at break point at both tensile and compressive sides (about five times ultimate strain, 6000 μm, of mortar). When this thin composite panel is subjected to bending, the loading and deflection increase continuously even after the occurrence of crack in the polymer mortar core due to the confinement and tensile reinforcement effect of GFRP at bottom and top, reaching the fracture of GFRP-reinforcement layer or the failure of the bond between GFRP and the polymer mortar core eventually. After the occurrence of crack at the polymer mortar core, various complex factors come into play. They are (1) strut formed by the polymer mortar to bear the compression after the occurrence of crack at the polymer mortar core and GFRP to bear the tension, (2) bonding of the polymer mortar at the tensile side and GFRP reinforcement, and (3) the confinement effect of GFRP reinforcement on polymer mortar core, etc. For these reasons, the theoretical analysis of the flexural behavior and final failure mechanism for thin sandwich panel members is very difficult.

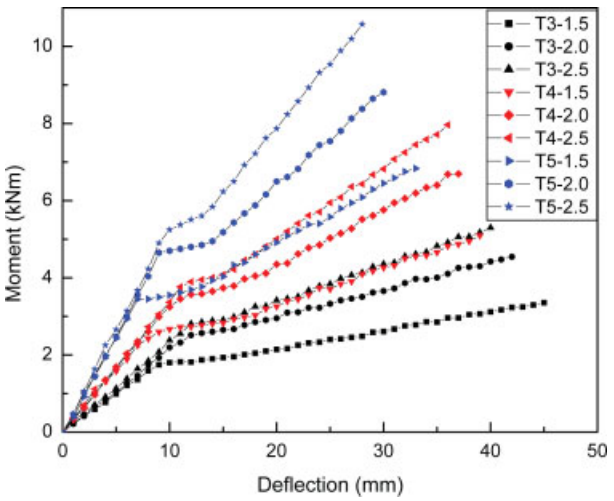

Figure 5 Moment-deflection curves for all specimens. [Color figure can be viewed in the online issue, which is available at www.interscience.wiley.com.]

Moment-deflection

Figure 5 illustrates the moment-deflection relationships for the polymer mortar sandwich panel specimens reinforced with GFRP with various thicknesses of the core and face. As it can be seen in the figure, the moment and deflection varied linearly together up until the occurrence of crack at the core. After crack took place, the stiffness of the panel decreased to exhibit bilinear behavior.

Prior to the crack, the entire cross-section of the polymer mortar core functioned effectively. Then, after the bottom part of the polymer mortar core cracked, the crack propagated gradually to the neutral axis to lower the stiffness, and deflection was markedly noticed due to the increased moment. Although the gradient of the moment-deflection curve was leveled more due to the lowered stiffness after the crack in the polymer mortar, the gradient of the curve was still inclining up until the yield moment. This could be anticipated from the stress–strain property of GFRP used as the reinforcement at the faces of the test speci-

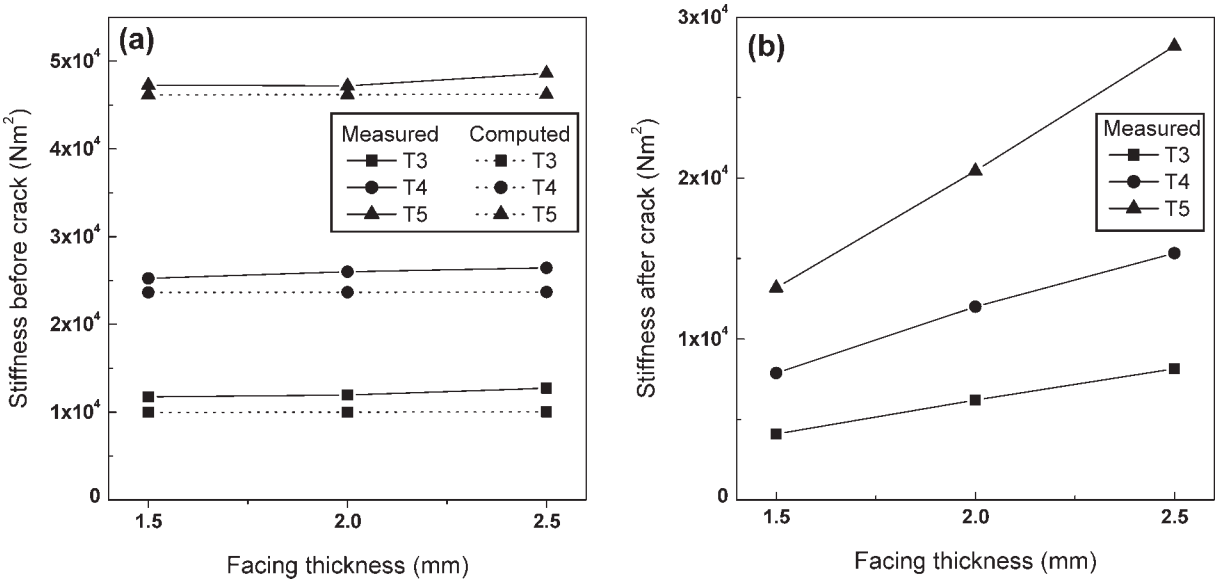

Figure 6 Stiffness of members (a) before cracking and (b) after cracking.

men. As Figure 4(b) shows, GFRP exhibited almost linear behavior even beyond a loading greater than 40–50% of the ultimate load, and this behavior continued until the specimen was fractured.

Flexural stiffness

The flexural stiffness (EI) can be expressed as the ratio of the flexural moment to the curvature (M/ψ) within the range of elastic behavior of the specimen before crack takes place at the polymer mortar in the core of the sandwich panel. Flexural stiffness is an index to indicate how much strain is exerted on the member subjected to a uniform load from outside, and it is a very important structural parameter.

The flexural stiffness (E_1I_1) of the sandwich panel prior to cracking can be expressed as in eq. (1)[23]:

$$E_1I_1 = \frac{E_f b t_f}{6}(3t_c^2 + 6t_f t_c + 4t_f^2) + \frac{E_{\mathrm{pm}} b t_{\mathrm{pm}}^3}{12}, \qquad (1)$$

where, E_1 is the elastic modulus of the flexural member (Pa), I_1 is the moment of inertia (m^4), E_f is the tensile modulus of elasticity of GFRP (N/m^2), $t_f(t_c)$ is the thickness of GFRP at the tensile (compressive) side (m), E_{pm} is the elastic modulus of the polymer mortar (N/m^2), t_{pm} is the thickness of the polymer mortar core (m), and b is the width of the test specimen (m).

Additionally, the gradient of an arbitrary point on the moment-curvature curve before or after cracking is the same as the flexural stiffness of the member at that point.[13] At this time, the curvature (ψ) can be obtained from the strain measured by the strain gauges installed at the compressive and tensile side during the flexural test, and the flexural stiffness at a random point (i) can be expressed as the following eq. (2):

$$(EP)_i = \frac{M}{\psi_i} = \frac{MT}{|\varepsilon_{1i}| + |\varepsilon_{2i}|}. \qquad (2)$$

In this equation, $\psi_i = (|\varepsilon_{1i}| + |\varepsilon_{2i}|)/T$ is the curvature at an arbitrary point ε_{1i}, ε_{2i} are the strains on GFRP at an arbitrary point (i) on the compressive and tensile side, respectively, and T is the thickness of the test specimen.

Figure 6(a) shows the flexural stiffness as computed from an elasticity theory and as measured from moment-curvature relationship of the experimental data prior to the occurrence of crack. It shows that the measured values for the flexural stiffness of polymer mortar sandwich panel reinforced with GFRP prior to the occurrence of crack at the polymer mortar core were greater than the theoretically computed value, when the values for flexural stiffness were compared between the computed value based on the elasticity theory and the measured value from moment-curvature relationship of the experimental data prior to the occurrence of crack.

Prediction of the deflection after the occurrence of crack

The computation of flexural stiffness is determined by the elastic modulus of the material, the shape and size of the member within the range of elastic behavior of the specimen. Because the elastic modulus of the material is a constant for the material and the moment of inertia is effective for the total cross section within the range of elastic behavior of the specimen, the exact

computation of flexural stiffness is possible by using the total moment inertia. However, because that the moment of inertia outside the range of elastic behavior of the specimen changes, the computation of flexural stiffness becomes very complex and difficult.

Effective moment model. Many methods to predict the deflection of reinforced concrete members were found to be inappropriate for the concrete specimens reinforced with FRP bars.[24–26] According to ACI Building Code[4] and Canadian Building Code,[5] the deflection of reinforced concrete members after the occurrence of crack can be computed by the following formula for the effective moment of inertia:

$$I_e = I_{\mathrm{cr}} + (I_g - I_{\mathrm{cr}})\left(\frac{M_{\mathrm{cr}}}{M_a}\right)^3 \le I_g, \tag{3}$$

where, M_a is the maximum moment of the member for which the deflection is computed, M_{cr} is the crack resistance moment, I_g is the second moment of the cross section for the entire concrete cross-section excluding reinforcing steel, and I_{cr} is the transformed moment of inertia of the cracked cross-section.

This study revised existing equations to predict the deflection and applied it by considering the small elasticity of GFRP and the formation, shape, and propagation of cracks. In general, the members with cracks have the stiffness of the member decrease after the crack, and their cross section does not behave like a ductile member. The polymer mortar does not have adequate tensile stress during the occurrence of crack. However, the core affects the flexural stress of the member to exhibit a tension stiffening effect just like a reinforced concrete while cracking takes place in the core. This study introduces models to explain the tension stiffening effect for the polymer mortar bar reinforced with GFRP besides the aforementioned methods to predict deflection of reinforced concrete. The models, which revised the effective moment of inertia, such as ACI Committee 440 model,[6] mean moment of inertia model,[9] bilinear model,[12] etc., are such models to predict the deflection after the crack occurrence. The deflection of the specimens is computed using these models, and the computed values are to be compared with the results of this experimental study.

ACI Committee 440 model. ACI Committee 440 model[6] is used as a guideline for the design of concrete structures reinforced with FRP bars. According to this guideline, the instantaneous deflection due to loading can be computed from the effective moment of inertia. That is,

$$I_e = I_{\mathrm{cr}} + (\beta I_g - I_{\mathrm{cr}})\left(\frac{M_{\mathrm{cr}}}{M_a}\right)^3 \le I_g, \tag{4}$$

where, $\beta = \alpha(E_f/E_s + 1)$, E_f is the elastic modulus of FRP, E_s is the elastic modulus of reinforcing steel, α is the coefficient related to the bonding between FRP bar and concrete and has the same value of 0.5 as the steel bar for the case of GFRP bar.[7,27] Although β is a parameter related to bonding and elastic modulus of FRP bar, this study computed it by setting $\alpha = 0.5$ for the reason that the elastic modulus of the steel bar is greater than that of FRP, that is, $E_f/E_s \approx 0.05$.

Mean moment inertia. This method was first introduced by Hall and Ghali[9] to predict the instantaneous short-term deflection right after the occurrence of crack in the beam reinforced with GFRP bars and long-term deflection after the crack in the GFRP-reinforced beam. This method computes the deflection by integrating the area under the mean curvature through entire section of the member at the middle point of span. Average curvature is given by $\psi_m = M/EI_m$, where M is the moment exerted at an arbitrary section of the member, E is the elastic modulus of the member, and I_m is the mean moment of inertia given by the following equation. That is,

$$I_m = \frac{I_1 I_2}{I_1 + \beta_1\beta_2\left(\frac{M_{\mathrm{cr}}}{M_a}\right)^2 (I_2 - I_1)}, \tag{5}$$

where, I_1 and I_2 is the transformed moment of inertia prior to and after the occurrence of crack, respectively. β_1 is the coefficient related to reinforcing bars and has the value of 1.0 for the case of high-bond bars and 0.5 for the case of smooth bars. β_2 is the coefficient related to continuous or repetitive loading and has the value of 0.8 for initial loading and 0.5 for continuous or repetitive loading.[9] To simplify the computation, this study computed the deflection at the center of the distance interval using the curvature at the center section of the member as suggested by Hall and Ghali.[9] That is, when the curvature at the center is ψ_c, the deflection of the simply supported member (Δ) with the span l is computed by the following equation[9]:

$$\Delta = \frac{5l^2}{48}\psi_c. \tag{6}$$

Bilinear method. Following CEB-FIP Model Code 1990,[12] Favre and Charif[13] proposed the following instantaneous deflection equation to compute the deflection of ordinary reinforced concrete. That is,

$$\Delta = \Delta_2 - (\Delta_2 - \Delta_1)\beta\frac{M_{\mathrm{cr}}}{M_a} \tag{7}$$

where, Δ_1 and Δ_2 are the deflection prior to and after the occurrence of crack, respectively, while not considering tension stiffening effect. $\beta = \beta_1\beta_2$, where the entire term, $(\Delta_2 - \Delta_1)\beta(M_{\mathrm{cr}}/M_a)$, indicates the tension stiffening effect of ordinary reinforced concrete.

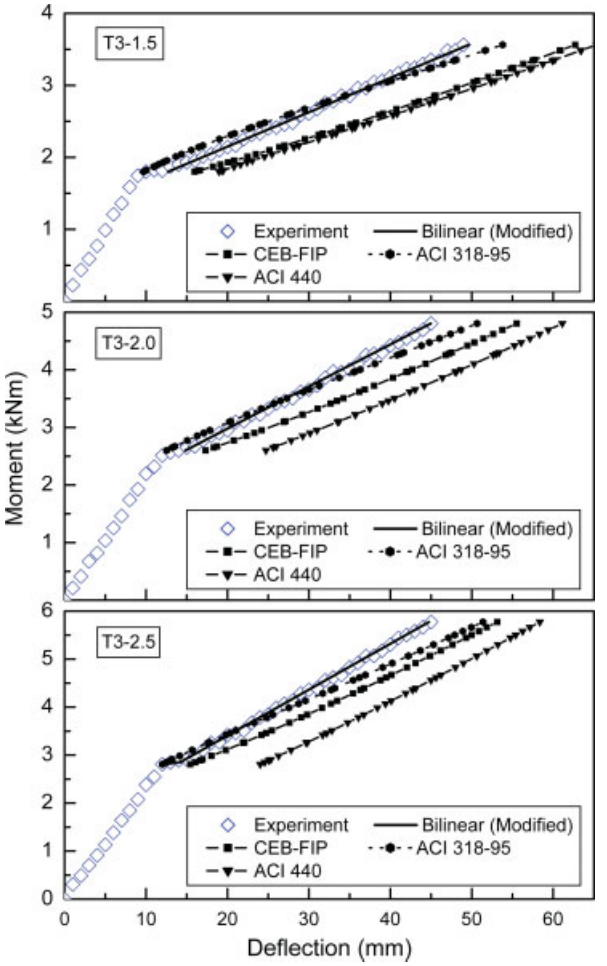

Figure 7 Comparison of experimental and computational deflection for core thickness of 30-mm specimens. [Color figure can be viewed in the online issue, which is available at www.interscience.wiley.com.]

The deflection prior to the occurrence of crack, Δ_1, can be easily predicted from a theory on flexural stiffness as shown in the following equation:

$$\Delta_1 = k_M l^2 \frac{M_a}{E_c I_1}. \quad (8)$$

Then, the deflection after the occurrence of crack can be expressed as the following equation:

$$\Delta = k_M l^2 \left(\frac{\beta M_a}{E_c I_1} + \chi \frac{M_a - \beta M_{cr}}{E_c I_{cr}} \right) \quad (9)$$

where, k_M is a constant determined by loading method and bearing condition, l is span of the member, and E_c is the elastic modulus of polymer mortar. β is a coefficient describing the tension stiffening effect on the member. When eq. (9) was fitted to the experimental results, the value for β in eq. (9), which was the closest to the experimental result, was 0.8 regardless of the thickness at the core or the face in compliance with the prediction of the Ref. 13. The tension stiffening effect was observed constantly regardless of the thickness of the sandwich panel specimen at the core or the face in this study. χ is an important element to indicate the stiffness of the member or the gradient of the moment-deflection or moment-curvature curve after the occurrence of crack. Unlike the previously reported case of steel or FRP bar reinforcement,[28] this study for the case of polymer mortar reinforced with GFRP slab revealed that the value of χ differed with the thickness of the specimen at the core and the face.

Figures 7–9 compare the measured moment-deflection values from the experiment and computed moment-deflection values from prediction models for three cases of the core thickness of 30, 40, and 50 mm, respectively. As it can be seen in the figures, ACI-318-95 model computed similar deflection values for all core thicknesses, but there were some differences in the gradient of the moment-deflection curve. On the other hand, CEB-FRP model, which assumed $\beta_1\beta_2 = 0.8$, predicted greater deflection

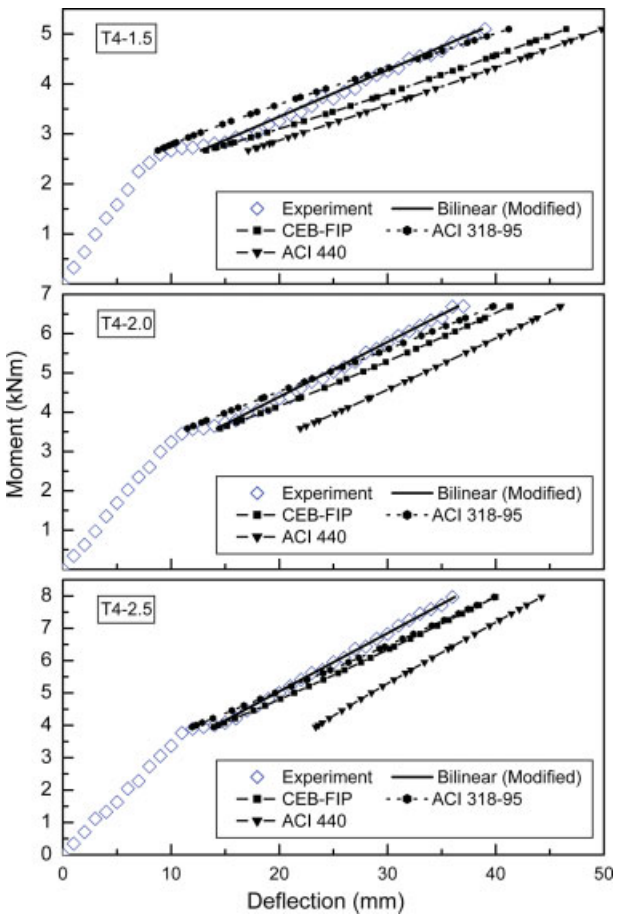

Figure 8 Comparison of experimental and computational deflection for core thickness of 40-mm specimens. [Color figure can be viewed in the online issue, which is available at www.interscience.wiley.com.]

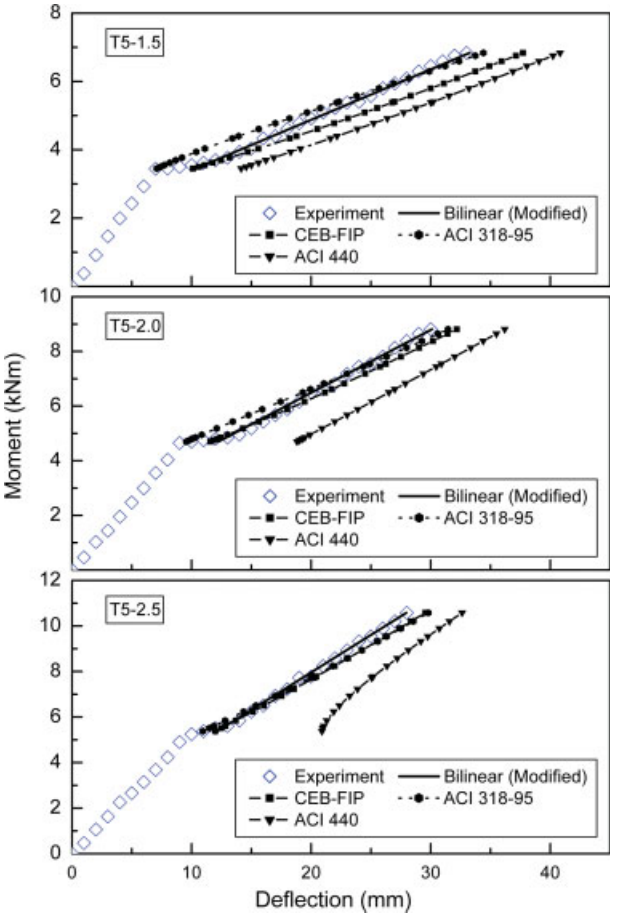

Figure 9 Comparison of experimental and computational deflection for core thickness of 50-mm specimens. [Color figure can be viewed in the online issue, which is available at www.interscience.wiley.com.]

than the measured deflection, and the gradient of the moment-deflection curve was smaller than the measured value from the experiment. The ACI 440 model, which assumed $\beta = 0.8$ and $\alpha = 0.5$ predicted almost the same gradient value as the experimental value, but it computed the deflection values much greater than other models.

After the bilinear method was modified somewhat, the predictive power of the modified model was compared with the experimental results. Although the modification factor, χ, differed slightly with the thickness of the specimen at the core and the facings, the predicted values from the modified model were generally in congruence with the experimental results. The modification factor, χ, was in the range of $1.5 \leq \chi \leq 1.7$, and its average was 1.62. It is assumed that the reason the modification factor χ is in a certain predictable range of values is not due to the physical property of the specimen but due to the experimental environment. Previous research along with this study, in which the modification factor was multiplied to the second term of the right side of eq. (9) to apply the modified model successfully to concrete members reinforced with FRP bars, can be found.[28] The test specimen used in this study had the elastic modulus of the core greater than that of GFRP reinforcement at the face, and its bonding between the core and the facings was excellent unlike other sandwich panels with the elastic modulus of the core less than that of the reinforcement layer. It is assumed that it was for these reasons that the stiffness prior to and after the occurrence of crack showed to be greater than the stiffness predicted by theoretical models.

CONCLUSIONS

The moment-deflection relationship prior to and after the occurrence of crack was investigated by simple flexural bearing tests for nine test specimens of different thickness of the core and the face. The structure of the test specimens was polymer mortar sandwich panel reinforced with GFRP. The experimental results were then compared with existing deflection prediction models to derive the following conclusions.

The nine kinds of polymer mortar sandwich panels reinforced with GFRP, which were prepared for this study, exhibited linear moment-deflection relationship during the flexural test until the occurrence of crack. Although the flexural stiffness obtained from this experiment was generally higher than the theoretically predicted values, it concurred with the theoretical values in accordance with the thickness of the core and the reinforcement layer. Although the linear behavior continued due to the physical property of GFRP even after the occurrence of crack, the flexural stiffness decreased.

Such models as CI 318-95, ACI 440, CEB-FIP, bilinear model, etc., to predict the moment-deflection after the occurrence of crack in reinforced concrete were compared against the flexural tests on nine test specimens of different thickness at the core and the face. ACI-318-95 model computed almost the same values as the experimental results for all nine specimens, but there were some difference in the gradient of the moment-deflection curve. On the other hand, the computed deflection values from CEB-FRP model were greater than experimental values, while the gradient of the moment to deflection curve was smaller than that of experimental result. The gradient of ACI 440 model concurred with the experimental values in general, but its predicted deflection values were markedly greater than the deflection values predicted from other models.

A modification factor was introduced to the existing bilinear model, and the predicted deflection values from the revised model were compared against the experimental results. The theoretically computed

values concurred well with the experimental values. It is found that the modification factor is necessary due to the difference in crack mechanism such as the transformed moment of inertia after the occurrence of crack, because the bond between polymer mortar and GFRP of the sandwich panel is different from the case of steel concrete.

Polymer mortar sandwich panel reinforced with GFRP can be applied to the structural members those require high toughness and flexural strength. For example, one of the authors of this article designed GFRP pipe and took out a patent for an invention. The GFRP pipe for the sewer pipe is now being massively manufactured by a local company. Other possible applications are, for instance, the deck for small bridge, open-channel flume, etc.

This research was supported by Construction Core Technology Development Program (2002 Academic-Industry Cooperative Research Program B 01-03 and 2003 Academic-Industry Cooperative Research Program A 10-02) of Korea Institute of Construction and Transportation Technology Evaluation and Planning (KICTTEP) under the auspice of the Ministry of Construction and Transportation, and partially supported by Research Center for Advanced Mineral Aggregate Composite Products.

References

1. Zenkert, D., Ed. The Handbook of Sandwich Construction. EMAS Publishing: London, 1997.
2. Uddin, N.; Fouad, F.; Uday, K. V.; Khotpal, A.; Serrano-Perez, J. C. J Reinforced Plast Compos 2006, 25, 981.
3. Cosenza, E.; Carlo Greco, C. Mater Struct 1990, 23, 196.
4. ACI Committee 318. Building code requirements for reinforced concrete and commentary (ACI 318-89/ACI 318R-89). American Concrete Institute: Detroit, 1989.
5. CSA Standard CAN-A23.3-94. Design of concrete structures. Canadian Standards Association: Rexdale, Ontario, 1994.
6. ACI Committee 440. Guide for the design and construction of concrete reinforced with FRP bars. American Concrete Institute: Detroit, 2001; p 1023.
7. Pecce, M.; Manfredi, G.; Cosenza, E. J Compos Construct ASCE 2000, 4, 182.
8. Pesic, N.; Pilakoutas, K. Simplified design guidelines for FRP reinforced concrete beams in flexure. In: Proceeding of the 5th International Conference on Fibre-Reinforced Plastics for Reinforced Concrete Structures, FRPRCS-5, July 2001, Cambridge, UK, 2001; p 177.
9. Hall, T.; Ghali, A. Can J Civil Eng 2000, 27, 890.
10. Razaqpur, A. G. Provisions of the Canadian standard for the design of FRP reinforced concrete building components. In: Proceeding of the 3rd International Conference on Advanced Composite Materials in Bridges and Structures 2000, Ottawa, Canada 2000; p 865.
11. Razaqpur, A. G.; Sevecova, D.; Cheung, M. S. ACI Struct J 2000, 97, 185.
12. Comité Euro-International du Béton-Fédération Internationale de la Précontrainte, CEB-FIP Model Code 1990. Thomas Telford, London, 1993.
13. Favre, R.; Charif, H. ACI Struct J 1994, 91, 169.
14. BS 6319-1:1983. Testing of resin and polymer/cement compositions for use in construction. Method for preparation of test specimens; The British Standards Institute: London, 1983.
15. BS 2782-9:Methods 920A to 920C:1977. Methods of testing plastics. Sampling and test specimen preparation. Preparation of glass fibre reinforced, resin bonded, low-pressure laminated plates or panels for test purposes.
16. BS 6319-1:1983. Testing of resin and polymer/cement compositions for use in construction. Method for preparation of test specimens.
17. BS 6319-2:1983. Testing of resin and polymer/cement compositions for use in construction. Method for measurement of compressive strength.
18. BS 6319-3:1990. Testing of resin and polymer/cement compositions for use in construction. Methods for measurement of modulus of elasticity in flexure and flexural strength.
19. BS 6319-7:1985. Testing of resin and polymer/cement compositions for use in construction. Method for measurement of tensile strength.
20. BS 6319-6:1984. Testing of resin and polymer/cement compositions for use in construction. Method for determination of modulus of elasticity in compression.
21. BS 2782-9:Methods 920A to 920C:1977. Methods of testing plastics. Sampling and test specimen preparation. Preparation of glass fibre reinforced, resin bonded, low-pressure laminated plates or panels for test purposes.
22. JIS A1414. Method of performance test of panels for building construction.
23. Kuenzi, E. W. Structural sandwich design criteria, U.S. Dept. of Agriculture, Forest Service, Forest Products Laboratory Report 1959, No. 2161.
24. Faza, S. S.; Ganga Rao, H. V. S. In: Reinforced-Plastic Reinforcement for Concrete Structures, SP-138; Nanni, A., Dolan, C. W., Eds.; American Concrete Institute: Detroit, 1993; p 599.
25. Abdalla, H. A.; El-Badry, M. M.; Rizkalla, S. H. Deflection of concrete slabs reinforced with advanced composite materials. In: Proceeding of the 2nd International Conference on Advanced Composite Materials in Bridges and Structures 1996; Montreal, Canada, 1996; p 201.
26. Toutanji, H. A.; Saafi, M. In: Fibre Reinforced Polymer Reinforcement for Concrete Structures, SP-188. American Concrete Institute: Detroit; 1999; p 133.
27. Pesic, N.; Pilakoutas, K. Simplified design guidelines for FRP reinforced concrete beams in flexure. In: Proceeding of the 5th International Conference on Fibre-Reinforced Plastics for Reinforced Concrete Structures, FRPRCS-5 2001; Cambridge, UK, 2001; p 177.
28. Abdalla, H. A. Compos Struct 2002, 56, 63.